Corrigendum : Extended Magneto-Hydro-Dynamic model for Neoclassical Tearing Mode Computations

Patrick Maget, Olivier Février, Xavier Garbet, Hinrich Lütjens, Jean-François Luciani, Alain Marx

Corrigendum : Extended Magneto-Hydro-Dynamic model for Neoclassical Tearing Mode Computations

Patrick Maget , Olivier Février[2], Xavier Garbet, Hinrich Lütjens[1], Jean-Francois Luciani[1], Alain Marx[1]

CEA, IRFM, F-13108 Saint Paul-lez-Durance, France.

[1]Centre de Physique Théorique, Ecole Polytechnique, CNRS, France.

[2]SPC, Ecole Polytechnique Fédérale de Lausanne, CH-1015 Lausanne, Switzerland.

E-mail: patrick.maget@cea.fr

An extended fluid model covering neoclassical physics has been implemented in the XTOR code for Magneto-Hydro-Dynamic computations and is described in [1]. This model allows recovering neoclassical flux average quantities like the bootstrap current and the poloidal ion flow, and in the presence of a magnetic island, it generates a drive for Neoclassical Tearing Modes. The contribution of parallel heat fluxes on the bootstrap current is significant, and it was retained in the simulations presented in this paper. However, we have realized that the closure that is used for these parallel heat fluxes does not meet an important constraint on its spatial distribution, and although this does not change the equilibrium quantities, we do see an impact on the dynamics of the magnetic island. In the following, we propose a different closure that satisfies this constraint, and we also present a slight modification of the neoclassical implementation in the momentum equation. In order to show how these modifications impact the simulations, we present a limited number of examples performed with the new model, with diagnostics tools allowing a better understanding of the physics at play.

1. Corrections to the MHD model

1.1. Closure on parallel heat fluxes

The modifications that we report here concerns the expression of parallel heat flows and the momentum equation. The parallel heat flux of the species a can be expressed as a function of plasma flows and neoclassical forces from each species b. The flux average parallel heat flux satisfies :

$$\left\langle u_{2\|a} \right\rangle = \sum_b \left\langle \left[C_\|^{ab} u_{1\|b} + C_1^{ab} S_1^b + C_2^{ab} S_2^b \right] \right\rangle \tag{1}$$

with $u_{1\|b} \equiv \mathbf{V_b} \cdot \mathbf{B}$ and $u_{2\|a} \equiv 2\mathbf{q_a} \cdot \mathbf{B}/(5p_a)$. The expressions for $C_\|^{ab}$, C_1^{ab} and C_2^{ab} are given in the appendix of reference [1]. The terms $S_{1,2}^b$ need however some modification. Indeed, the expressions given in reference [1] have a dependence in $\sin^2\theta$ with θ the poloidal angle, due to the poloidal variation of the magnetic field amplitude as $\cos\theta$.

Since we have no evolution equation for the heat flux $u_{2\|a}$, this strong poloidal variation cannot be regularized and leads to unphysical poloidal distribution of the parallel heat flux. In order to solve this difficulty while maintaining the correct flux averaged relation that leads to the equilibrium bootstrap current, we adopt the following definitions :

$$\begin{pmatrix} S_1^a \\ S_2^a \end{pmatrix} = \frac{B^2}{\mathbf{B}\cdot\nabla\theta} \begin{pmatrix} \mathbf{V_a^*} + \mathbf{V_E} \\ \mathbf{V_{Ta}^*} \end{pmatrix} \cdot \nabla\theta \tag{2}$$

with $\mathbf{V}_{Ta}^* = \mathbf{B}\times\nabla T_a/(e_a n_a B^2)$, with a perpendicular heat flux given by

$$2\mathbf{q_{a\perp}}/(5p_a) = \mathbf{V_{Ta}^*} \tag{3}$$

The closure on the parallel heat flux is then derived from equilibrium constraints. It can be written as

$$u_{2\|a} = \frac{2}{5p_a}\frac{\mathbf{q_a}\cdot\nabla\theta}{\mathbf{B}\cdot\nabla\theta}B^2 - S_2^a \tag{4}$$

At equilibrium, assuming that the heat flux is divergence free and has no radial component, we have

$$\partial_\theta\left(\frac{\mathbf{q_a}\cdot\nabla\theta}{\mathbf{B}\cdot\nabla\theta}\right) = 0 \tag{5}$$

so that this quantity is a flux function. It is also easily shown that S_2^a is a flux function at equilibrium, so that we can write

$$u_{2\|a} = \frac{\langle u_{2\|a}\rangle B^2}{\langle B^2\rangle} + \left(\frac{B^2}{\langle B^2\rangle} - 1\right) S_2^a \tag{6}$$

We will use this relation as the closure on the parallel heat flux. The contribution of the heat flux in the pressure anisotropy (see equation (29) of [1]) is therefore :

$$\left(\mathbf{V}_{Ta}^* + \frac{u_{2\|a}}{B^2}\mathbf{B}\right)\cdot\nabla\theta = \frac{B^2}{\langle B^2\rangle}\mathbf{V}_{Ta}^*\cdot\nabla\theta + \frac{\langle u_{2\|a}\rangle}{\langle B^2\rangle}\mathbf{B}\cdot\nabla\theta \tag{7}$$

This formulation gives therefore the correct contribution of the flux averaged parallel heat fluxes but ignores how these fluxes can participate in the neoclassical island drive.

1.2. Momentum equation

Regarding the ion neoclassical friction force in the momentum equation, we used the following expression in [1] :

$$\nabla p + \nabla\cdot(\Pi_i + \Pi_e) = \left(p_\| - p_\perp\right)\left[(\nabla\cdot\mathbf{b})\,\mathbf{b} + \boldsymbol{\kappa}\right] + \nabla_\|\left(p_\| - p_\perp\right) + \nabla p_\perp \tag{8}$$

with $p = p_i + p_e$. This formulation remains satisfactory for moderate anisotropy where $p_\perp$ can be identified with p. However, this modification has proved to be unnecessary from a computation performance point of view, so that we now adopt the expression

$$\nabla\cdot(\Pi_i + \Pi_e) = \left(p_\| - p_\perp\right)\left[(\nabla\cdot\mathbf{b})\,\mathbf{b} + \boldsymbol{\kappa}\right] + \nabla_\|\left(p_\| - p_\perp\right) - \frac{1}{3}\nabla\left(p_\| - p_\perp\right) \tag{9}$$

that allows better comparison with formal derivations of neoclassical island theory (as in [2] for example).

2. Measure of neoclassical contribution

In order to characterize the neoclassical drive in a simple way, we define a scalar $R(f,g)$ that quantify the correlation between two 3D fields f and g over the plasma volume V :

$$R(f,g) = \left(\int dV fg\right) / \left[\left(\int dV f^2\right)^{1/2} \left(\int dV g^2\right)^{1/2}\right] \tag{10}$$

This scalar is unity if f is proportional to g with the same sign, and minus unity if the sign is opposite. If the two fields are completely uncorrelated, $R(f,g)$ should be close to zero.

The link between the bootstrap current perturbation and the pressure gradient perturbation can then be evaluated by taking $f \equiv [J_{bs,\varphi}]_{n\neq 0}$ and $g(h) \equiv [-\partial_y h]_{n\neq 0}$, using $h = p$ (pressure), T (temperature), or ρ (density), $y \equiv \sqrt{\psi}$ the radial co-ordinate and n the toroidal mode number. In the following, we note $R_{bs}(h) = R(f, g(h))$. In order to quantify the contribution of the perturbed $\mathbf{E}\times\mathbf{B}$ velocity $\mathbf{V_E}$, we also compute $R_{bs}(v) = R(f,g)$ with $g = [V_{E,\theta}]_{n\neq 0}$. Although the bootstrap current can be formally expressed as a sum of the contributions from $g(p)$, $g(\rho)$ and $g(v)$, note that the sum of their correlation terms R_{bs} is not constrained to be unity.

In the evaluation of the bootstrap drive to island growth, it is generally assumed that the neoclassical friction is strong enough to force the perturbed flow to its neoclassical drive. This motivates the use of an ad-hoc bootstrap model where $J_{bs} \propto -\nabla p$ for non linear simulations of NTM dynamics [3, 4, 5, 6]. With such a model, we have naturally $R_{bs}(p) \equiv 1$ and a bootstrap perturbation that is closely linked to the island structure, due to the large parallel diffusivity that equilibrates the temperature along magnetic field lines.

3. Numerical simulations

We have performed numerical simulations on the same equilibrium that was used in [1], with an ion density $n_i(0) = 2\times 10^{19} m^{-3}$, electron temperature $T_e(0) = 3910eV$, and $\tau \equiv T_i/T_e = 1$, a Lundquist number $S_0 = 10^7$, a magnetic Prandtl number Prm$\equiv \nu/\eta = 10$, $\chi_\parallel/\chi_\perp = 10^8$, $\chi_\perp/\eta = 150$, and $D_\perp = 2/3\chi_\perp$.

In oder to save computation time, a (2,1) seed island is inserted at the beginning of the simulation, with a size $W = 4\%$. The evolution of the island width, the bootstrap current fraction at the resonance and the correlations $R_{bs}(p)$ and $R_{bs}(v)$ are shown in figure 1 for different amplifications of the bootstrap current. The simulation for $f_{bs} = 1$ can be compared with figure 7 of [1]. Although the saturation size is similar, we note the absence of the island breaking events, similar to the sporadic growth of plasmoids, that were present with the previous closure. The scan in bootstrap current shows, as noted before, a weak effect that is even opposite to the usual destabilizing drive. This can be understood with the correlation between the bootstrap perturbation and the island structure $R_{bs}(p)$ that is slightly negative. On the contrary, the correlation $R_{bs}(v)$ is

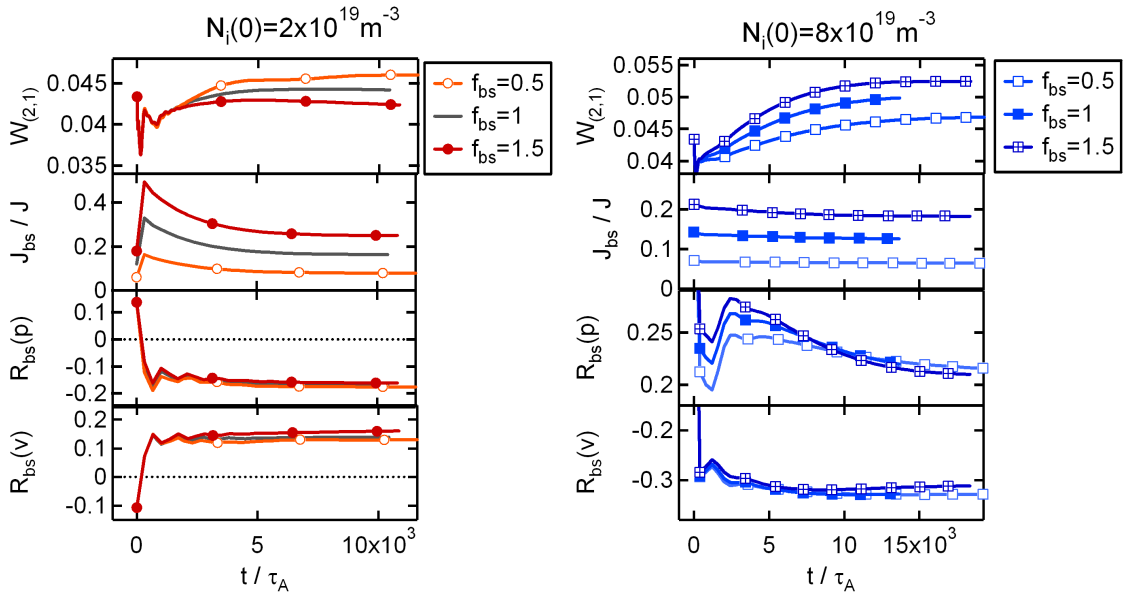

Figure 1. Influence of the bootstrap current on the island dynamics at low density (left, reference case), and high density (right), with f_{bs} the amplification factor. From top to bottom: island size, bootstrap current fraction at $q = 2$, correlation indicators $R_{bs}(p)$ and $R_{bs}(v)$.

slightly positive, showing that the contribution of the perturbed electrostatic potential in the bootstrap current is larger than that of the diamagnetic flows.

This result can be understood by the fact that temperature flattening inside the saturated island is small, thus limiting the nonlinear impact of the island on the bootstrap current. In the simulation, this temperature flattening is controlled by the characteristic transport width W_χ [7] defined in [1]. We have verified that the correlation $R_{bs}(p)$ increases when the characteristic width W_χ is reduced, as shown in figure 2 where it becomes slightly positive. Whereas W_χ was originally larger than the saturated island width ($W_\chi = 4.7\%$), it has been decreased to $W_\chi = 3.3\%$ by increasing the parallel diffusivity coefficient by a factor of 4. At the same time, the curvature stabilization effect is reinforced and reduces the island saturation [8].

But the insufficient temperature flattening is not the only mechanism causing the vanishing of the bootstrap drive that is observed in the simulation of figure 1. A strong contributor is found to be diamagnetic rotation, that opposes diffusive processes in the equilibration of temperature along field lines. For changing the level of diamagnetic rotations without modifying the magnetic equilibrium, we increase plasma density, and decrease temperature accordingly to keep the same pressure. By doing so, we also modify the bootstrap current and the neoclassical friction coefficients (see table 1). The amplitude of this friction term is expected to be crucial for the neoclassical drive following [9, 10] where a characteristic width $W_\nu \propto (\nu/\mu_i)^{1/2}$ was introduced. With our

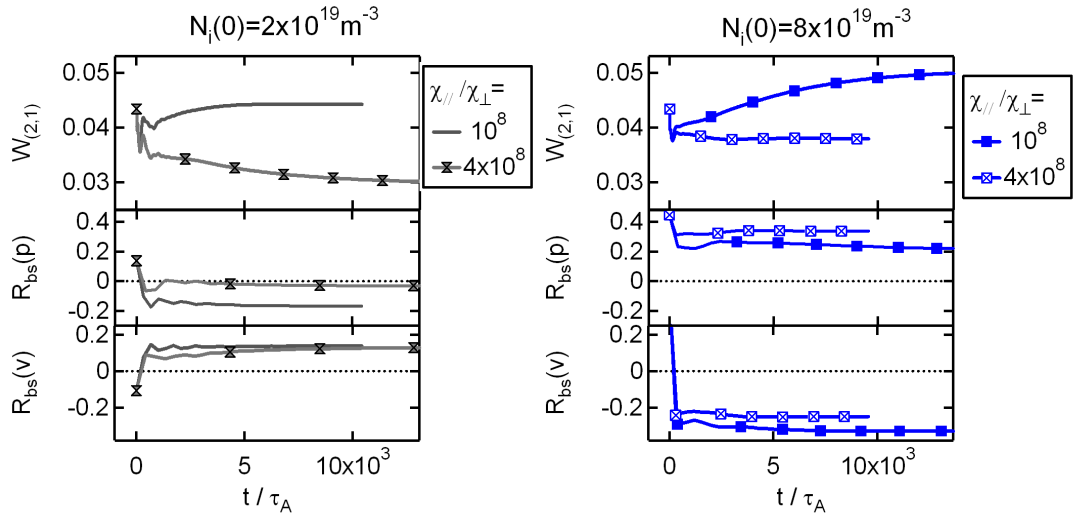

Figure 2. Influence of the characteristic transport width W_χ on the island dynamics at low density (left, reference case), and high density (right), with $W_\chi = 4.7\%$ for $\chi_\parallel/\chi_\perp^0 = 10^8$ and $W_\chi = 3.3\%$ for $\chi_\parallel/\chi_\perp^0 = 4\times10^8$ ($\chi_\perp^0$ is the value of $\chi_\perp$ at plasma center, and it is about a factor two above at $q = 2$). From top to bottom: island size, correlation indicators $R_{bs}(p)$ and $R_{bs}(v)$.

notations and normalizations, this width is given by:

$$W_\nu^{real} = \frac{1}{2}\left(\nu/\mu_i\right)^{1/2} = \frac{1}{2}\mathrm{Prm}^{1/2}\left(\mathrm{S}^{\mathrm{real}}\mu_\mathrm{i}\right)^{-1/2} \tag{11}$$

In our simulations, we do not rescale the ion neoclassical friction term μ_i with the Lundquist number, but we have the possibility to scale it by a factor α_μ. We have therefore

$$W_\nu^{sim} = \left(\frac{S^{real}}{S_0\alpha_\mu}\right)^{1/2} W_\nu^{real} \tag{12}$$

The values for W_ν^{real} and W_ν^{sim} corresponding to the simulations are reported in table 1. While in real situations the visco-neoclassical width is weakly sensitive to the scan in density that we have performed, a wide range is covered in the simulations, mainly due to the variation of the real Lundquist number. In particular, the ion neoclassical friction coefficient is increased by one order of magnitude between the cases $N_i(0) = 2\times10^{19}m^{-3}$ and $N_i(0) = 8\times10^{19}m^{-3}$. By setting $\alpha_\mu = 10$ (or even $\alpha_\mu = 20$) in the reference case at $N_i(0) = 2\times10^{19}m^{-3}$, we reduce the visco-neoclassical width below the island width, but we remain still larger than the real one. In this range at least, the correlation parameter remains constant and negative (see figure 4), showing that the dominant effect seen in the simulations comes from the change of diamagnetic rotations. At a lower level of diamagnetic rotation, the pressure contribution to the bootstrap drive increases significantly (see figure 3). This is confirmed by the fact that the island saturation increases when the bootstrap current is amplified by the factor f_{bs} (see figure 1, right plot).

Case	S^{real} $[\times 10^7]$	$N_i(0)$ $[10^{19}m^{-3}]$	J_{bs}/J_0 at $q=2$	W_ν^{real}	W_ν^{sim}
Ref	75.8	2	0.22	0.016	0.140
Ref $f_{bs}=0.5$	75.8	2	0.11	0.016	0.140
Ref $f_{bs}=1.5$	75.8	2	0.33	0.016	0.140
Ref, $\alpha_\mu=10$	75.8	2	0.22	0.016	0.044
Ref, $\alpha_\mu=20$	75.8	2	0.22	0.016	0.031
$N_{ref}\times 2$	20.2	4	0.20	0.015	0.066
$N_{ref}\times 3$	9.3	6	0.18	0.016	0.047
$N_{ref}\times 4$	5.4	8	0.15	0.017	0.041
$N_{ref}\times 4$ $f_{bs}=0.5$	5.4	8	0.075	0.017	0.041
$N_{ref}\times 4$ $f_{bs}=1.5$	5.4	8	0.225	0.017	0.041

Table 1. Characteristic parameters (Prm=10, $S_0 = 10^7$ for the simulations): Lundquist number consistent with plasma parameters, central ion density, ratio of the equilibrium bootstrap current to the local current density at $q=2$, visco-neoclassical width consistent with plasma parameters and the one used in the simulations.

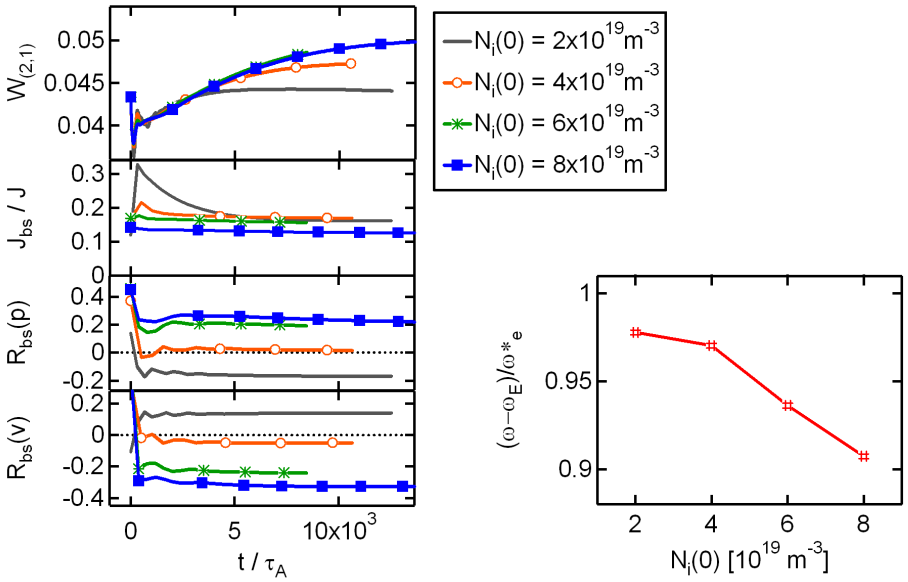

Figure 3. Influence of plasma density on the island dynamics. From top to bottom: island size, bootstrap current fraction at $q=2$, correlation indicators $R_{bs}(p)$ and $R_{bs}(v)$.

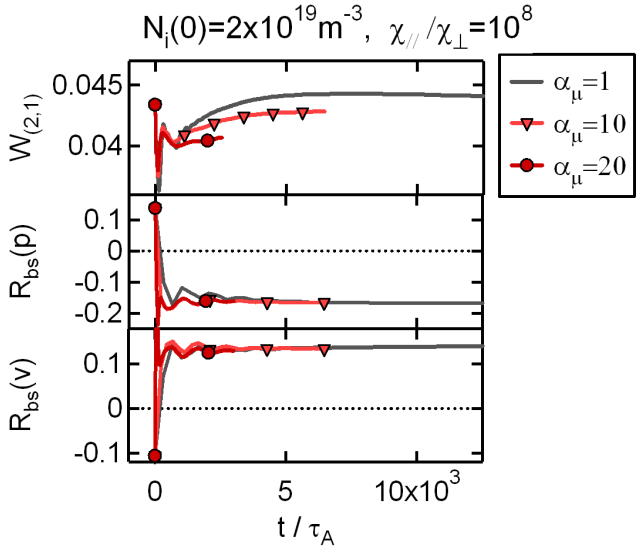

Figure 4. Influence of the visco-neoclassical width W_ν on the island dynamics for the reference case. We have $W_\nu = 14.0\%$ for $\alpha_\mu = 1$ and $W_\nu = 4.4\%$ for $\alpha_\mu = 10$. From top to bottom: island size, correlation indicators $R_{bs}(p)$ and $R_{bs}(v)$.

The series of simulations shown here demonstrate that we have now a neoclassical model that recovers qualitative expectations from theory, i.e. a bootstrap drive that increases the island saturation when it is sensitive to the island structure (positive $R_{bs}(p)$). The importance of the electrostatic contribution to the bootstrap current has been clearly evidenced when diamagnetic rotations are large enough, leading to a strong reduction of the bootstrap drive. The role of the visco-neoclassical width W_ν was not evidenced in the situation that we have encountered here, but it might be important in cases where the bootstrap drive is stronger.

In addition to the study of neoclassical tearing modes, this model also allows in a consistent approach to investigate the transport of impurities, following the generic mechanism involving the parallel friction force between the main ions and trace species [11].

Acknowledgments

This work has been carried out within the framework of the French Research Federation for Fusion Studies. We benefited from HPC resources from GENCI (project 056348) and from and from Marconi Aix-Marseille Université project Equip@Meso (ANR-10-EQPX-29-01) of the program "Investissements dAvenir" supervised by the Agence Nationale pour la Recherche. This work is part of the project AMICI funded by the Agence Nationale pour la Recherche (ANR-14-CE32-0004-01).

References

[1] Patrick Maget, Olivier Février, Xavier Garbet, Hinrich Lütjens, Jean-Francois Luciani, and Alain Marx. Extended magneto-hydro-dynamic model for neoclassical tearing mode computations. *Nuclear Fusion*, 56(8):086004, 2016.

[2] A. I. Smolyakov and E. Lazzaro. On neoclassical effects in the theory of magnetic islands. *Physics of Plasmas*, 11(9):4353–4360, 2004.

[3] Hinrich Lütjens, Jean-François Luciani, and Xavier Garbet. Nonlinear three-dimensional MHD simulations of tearing modes in tokamak plasmas. *Plasma Physics and Controlled Fusion*, 43(12A):A339–A348, 2001.

[4] Hinrich Lütjens and Jean-François Luciani. Linear and nonlinear thresholds of neoclassical tearing modes in tokamaks. *Physics of Plasmas*, 9(12):4837–4840, 2002.

[5] A. M. Popov, R. J. La Haye, Y. Q. Liu, M. Murakami, N. N. Popova, and A. D. Turnbull. Simulation of neoclassical tearing modes (NTMs) in the DIII-D tokamak. I. NTM excitation. *Physics of Plasmas*, 9(10):4205–4228, 2002.

[6] P. Maget, H. Lütjens, R. Coelho, B. Alper, M. Brix, P. Buratti, R.J. Buttery, E. De la Luna, N. Hawkes, G.T.A. Huysmans, I. Jenkins, C.D. Challis, C. Giroud, X. Litaudon, J. Mailloux, M. Ottaviani, and JET-EFDA Contributors. Modelling of (2,1) NTM threshold in JET advanced scenarios. *Nuclear Fusion*, 50(4):045004, 2010.

[7] Richard Fitzpatrick. Helical temperature perturbations associated with tearing modes in tokamak plasmas. *Physics of Plasmas*, 2(3):825–838, 1995.

[8] Hinrich Lütjens, Jean-François Luciani, and Xavier Garbet. Curvature effects on the dynamics of tearing modes in tokamaks. *Physics of Plasmas*, 8(10):4267–4270, 2001.

[9] S V Konovalov, A B Mikhailovskii, T Ozeki, T Takizuka, M S Shirokov, and N Hayashi. Role of anomalous transport in onset and evolution of neoclassical tearing modes. *Plasma Physics and Controlled Fusion*, 47(12B):B223, 2005.

[10] A.B. Mikhailovskii, M.S. Shirokov, S.V. Konovalov, and V.S. Tsypin. An analytic approach to developing transport threshold models of neoclassical tearing modes in tokamaks. *Plasma Physics Reports*, 31(5):347–368, 2005.

[11] Jae-H Ahn, X Garbet, H Lütjens, and R Guirlet. Dynamics of heavy impurities in non-linear MHD simulations of sawtoothing tokamak plasmas. *Plasma Physics and Controlled Fusion*, 58(12):125009, 2016.